SHORT COMMUNICATION



Check for updates

Cannabicitran: Its unexpected racemic nature and potential origins

Jared S. Wood | William H. Gordon | Jeremy B. Morgan | R. Thomas Williamson [©]

Department of Chemistry and Biochemistry, University of North Carolina Wilmington, Wilmington, North Carolina, USA

Correspondence

R. Thomas Williamson and Jeremy B. Morgan, Department of Chemistry and Biochemistry, University of North Carolina Wilmington, Wilmington, NC 28409, USA.

Email: williamsonr@uncw.edu and morganj@uncw.edu

Funding information

Yousry and Linda Sayed Endowment

Abstract

Cannabicitran is a cannabinoid found in levels up to $\sim \! 10\%$ in commercial "purified" cannabidiol (CBD) extracts. The structure of this natural product was first reported more than 50 years ago. However, few studies have investigated cannabicitran or its origin despite the rapidly increasing interest in the use of cannabinoids for the treatment of a wide range of physiological conditions. Following on a recent detailed NMR and computational characterization of cannabicitran, our group initiated ECD and TDDFT studies aimed at unequivocally determining the absolute configuration of cannabicitran present in *Cannabis sativa* extracts. To our surprise, we discovered the natural product was racemic, raising questions around its presumed enzymatic origin. Herein, we report the isolation and absolute configuration of (-)-cannabicitran and (+)-cannabicitran. Several possible scenarios for production of the racemate in the plant and/or during extract processing are discussed.

KEYWORDS

cannabicitran, cannabinoids, CBT-C, DFT calculations, ECD, NMR, OR, TDDFT, VCD

1 | INTRODUCTION

Cannabinoids, isolated from the *Cannabis sativa* plant, have been utilized for medicinal purposes for thousands of years. Several cannabinoids have receptor interactions that are indicated for the modulation of pain, sleep, and mood disorders, while also exerting beneficial effects in pathological conditions such as inflammation, cancer, addiction, and epilepsy. Cannabinoids such as Δ^9 -tetrahydrocannabinol (Δ^9 -THC) and cannabidiol (CBD) are primarily extracted from *C. sativa* as single enantiomers, but Δ^9 -cis-THC is known to be scalemic³; in contrast, only the (–) enantiomer of *trans*-CBD is naturally

found in the plant.^{4,5} This paper will provide insight into configurational analysis of such cannabinoids.

Determining the absolute configuration of a molecule is a crucial component of a complete molecular characterization, especially in the pursuit of developing effective therapeutics. The infamous and familiar story of (\pm) -thalidomide, used as a sedative for the treatment of morning sickness in pregnant women before withdrawal from the market due to the correlation of its use and severe teratogenic effects, provided the first broad awareness of this issue. ^{6,7} Before its official recall, thalidomide had adversely affected approximately 10,000 infants, resulting in limb and bone abnormalities, and almost 50% of the

This is an open access article under the terms of the Creative Commons Attribution-NonCommercial-NoDerivs License, which permits use and distribution in any medium, provided the original work is properly cited, the use is non-commercial and no modifications or adaptations are made.

© 2023 The Authors. Chirality published by Wiley Periodicals LLC.

Chirality. 2023;1–9. wileyonlinelibrary.com/journal/chir

1520636x, 0, Downloaded from https://onlinelibrary.wiley.com/doi/10.1002/chir.23571 by University Of North Carolina Wilmington, Wiley Online Library on [30/05/2023]. See the Terms and Condition -and-conditions) on Wiley Online Library for rules of use; OA articles are governed by the applicable Creative Commons Licenso

affected infants had died. It was eventually determined that R-(+)-thalidomide produced the desired sedative effects, while S-(-)-thalidomide was responsible for the teratogenic effects.8 Further, it was discovered in 1994 that the racemization of thalidomide occurs in vitro and even more rapidly in vivo. 9,10 Thus, enantiomerically pure R-(+)-thalidomide cannot be administered without an immediate partial conversion into S-(-)-thalidomide, the teratogen. The thalidomide tragedy harshly demonstrated the importance of chirality in the context of drug development and stimulated the creation of the FDA. Other chiral pharmaceutical examples like Darvon® (dextropropoxyphene) and Novrad® (levopropoxyphene) provide further illustration of complementary enantiomers targeting completely different receptors and exhibiting unrelated physiological effects. Darvon® elicits analgesic effects, and Novrad[®] is prescribed as an antitussive. 11

Recent studies have shown that various secondary metabolites in nature are racemates or scalemic mixtures, despite literature precedence suggesting they are individual enantiomers. 12 In addition, there are many papers on chiral molecules lacking information on enantiomeric purity because these studies are predominantly concerned with other details such as isolation, biological activity evaluation, and structure elucidation. 13,14 These discoveries raise important questions concerning molecule biosynthesis, and why nature produces racemates or scalemic mixtures instead of pure enantiomers. It is noteworthy that some racemates are known to have synergistic effects which yield higher biological activities relative to their individual enantiomers; one recent example is melipatulinone, which is known to inhibit pancreatic lipase. 15 Naturally, investigation of cannabinoid enantiomers for such qualities is warranted given the extensive collection of chiral metabolites present in C. sativa.

In fact, opposite enantiomers of cannabinoids are known to bind individual receptors with vastly different affinities and oftentimes have high affinity to entirely different protein targets. Enantiomers of Δ^9 -cis-THC (1) and trans-CBD (2) (Figure 1) have been shown to exhibit differences in binding affinities towards the CB₁ and CB₂ receptors. For both receptors, (–)-1 displays stronger binding relative to (+)-1. Further, both enantiomers have significant binding affinities towards endocannabinoid degrading enzymes such as MAGL and ABHD6. Unnatural (+)-2 has been shown to bind strongly to CB₁ and CB₂, unlike the natural (–)-2, which is known to bind to other targets such as 5-HT_{1A}, multiple TRPs, and GPR55. The strong transfer of the

Our group recently reported a detailed NMR study of cannabicitran (CBT-C, 3, Figure 1), a well-known but previously undercharacterized cannabinoid.¹⁸ In an extension of that work, we sought to determine the

absolute configuration of natural CBT-C (3) and discovered that it displays no electronic circular dichroism (ECD) signal. This observation led us to hypothesize that natural CBT-C (3) is racemic. Our hypothesis was strengthened when facile separation of the enantiomers was achieved using high-performance liquid chromatography (HPLC) with a chiral stationary phase. Additional ECD experiments performed with the isolated enantiomers provided further evidence that natural CBT-C (3) exists as a racemate. Through the utilization of ECD experiments combined with advanced time-dependent density functional theory (TDDFT) calculations and vibrational circular dichroism (VCD) measurements with corresponding DFT computed spectra, the absolute configurations of (-)-3 and (+)-3 have been firmly established.

Current intellectual property on CBT-C (3) indicates a wide range of applications for the cannabinoid, including uses in sunscreen, skin care, headache treatments, and treatment of Alzheimer's disease. Additionally, studies by ElSohly et al. revealed that CBT-C (3) reduces intraocular pressure in rabbits. This work suggests involvement of the NAGly (GPR18) receptor, a known target of structurally related cannabinoids. Prior research demonstrated that the receptor is linked to modulation of physiopathological processes such as pain, metabolism, and cancer. 4-26

2 | EXPERIMENTAL PROCEDURES

2.1 | ECD/VCD/OR experiments

All UV measurements and ECD experiments for natural CBT-C (3) and the enantiomerically pure (±)-CBT-Cs ((-)-3, (+)-3) were performed on a ChirascanTM Plus circular dichroism spectrometer in acetonitrile using a 1 mm pathlength cell. Concentrations for UV and ECD experiments were adjusted to provide for $A \approx 0.65$ at 214 nm. Degrees were measured in (m°) across a wavelength range of 180-300 nm in increments of 1.0 nm. VCD Experiments were performed on a BioTools ChiralIR-2XTM VCD spectrometer equipped with a DualPEMTM accessory, using a 0.20 mm pathlength cell. All infrared (IR) and VCD spectra were acquired across a range of 930-1650 cm⁻¹; these spectra were acquired with a PEM wave retardation factor of $\lambda/4$. Concentrations for VCD experiments were adjusted to $c \approx 50 \text{ mg/mL}$ in chloroform-d. All ECD, IR, and VCD sample spectra were baselined and blank subtracted. Optical rotation (OR) experiments were performed on a Rudolph Research Analytical Autopol® III Automatic Polarimeter. A 50 mm pathlength cell was used, and concentrations were adjusted to $c \approx 0.25$ g/dL.

FIGURE 1 Structures for (\pm) - Δ^9 -cis-THC (1), (\pm) -trans-CBD (2), (\pm) -CBT-C (3), CBC* (4), (\pm) - Δ^9 -trans-THC (5), and CBGA (6). All compounds (excluding 3) are important CBT-C-related compounds that will be discussed later in the manuscript. *Note that CBC (4) is known to be either scalemic or racemic.

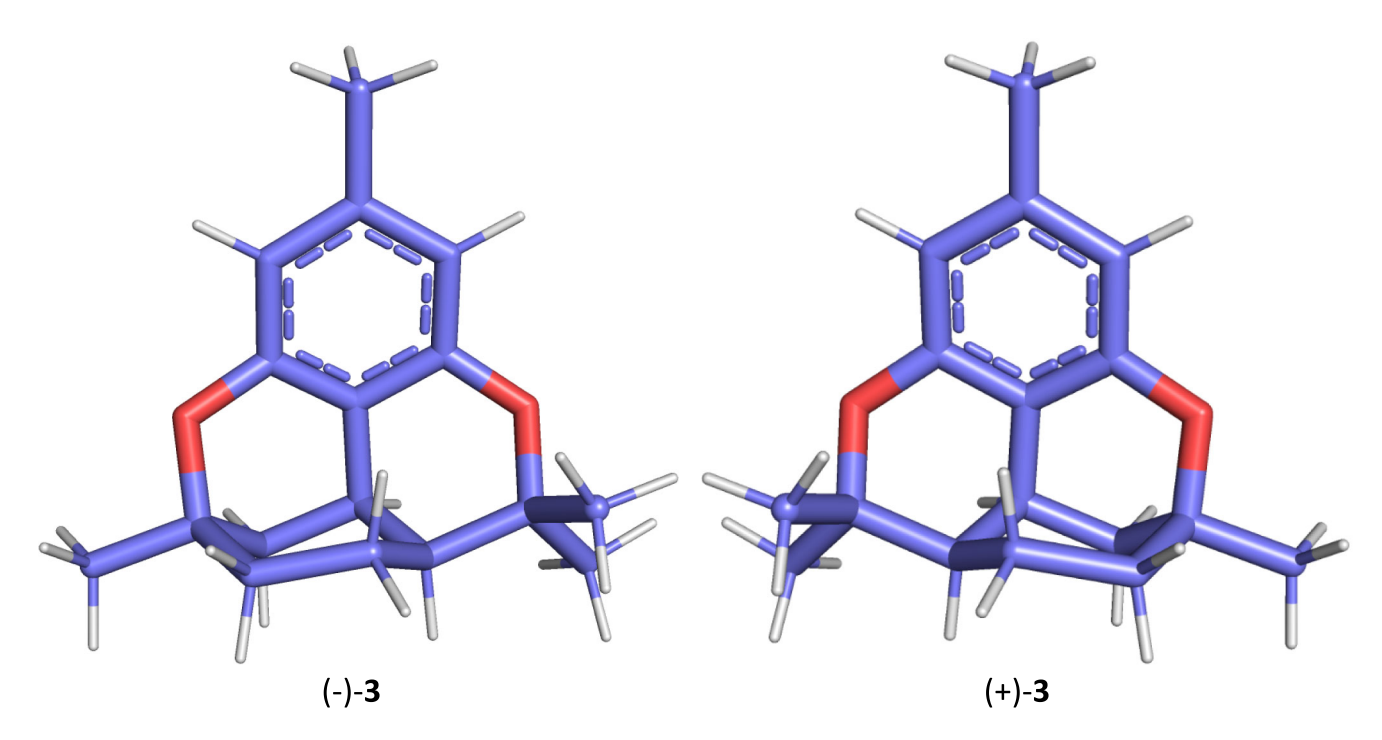


FIGURE 2 Truncated geometry-optimized 3D structures for both enantiomers of CBT-C (3).

2.2 | TDDFT calculations

In our previous NMR-based study of CBT-C (3), the Schrödinger MacroModel software package was used to mixed torsional/low-mode (MTLMOD) conformational search using the OPLS4 force field²⁷ on a methyl-truncated structure of (-)-3 (Figure 2). Geometry optimization and frequency calculations were performed on the primary conformer using the B3LYP/6-31G+(d,p) functional and basis set (gas phase). This optimized structure was used to predict OR and ECD data using the Gaussian software package through TDDFT calculations (see Supporting Information). The functionals and basis sets used for these calculations are shown below (Table 1). Three-dimensional models for the methyl-truncated enantiomers of CBT-C (3) are shown below (Figure 2).

All TDDFT calculations were repeated using the entire Boltzmann-weighted conformational ensemble of (–)-3 (152 conformers) at the ω B97XD/6-311G++(2d,2p) level of theory using an acetonitrile PCM solvent model to verify that there is negligible influence from the alkyl chain on the predicted ECD spectrum (see Supporting Information). In general, we recommend that TDDFT calculations for cannabinoids with olivetol-derived alkyl chains are performed using methyl-truncated structures.

Experimental and TDDFT-predicted UV and ECD data were processed and fitted in SpecDis.²⁸ All results

TABLE 1 Functionals and basis sets used in ECD, OR, and VCD predictions for CBT-C (3).

Data set	Functionals	Basis sets
ECD (100 excited states, 180.0–300.0 nm)	CAM-B3LYP ωB97XD	6-311G++(2d,2p) def2-TZVP aug-cc-pVTZ
OR (589.3 nm)	B3LYP CAM-B3LYP ωB97XD	6-311G++(2d,2p) def2-TZVP aug-cc-pVTZ
VCD (930-1650 cm ⁻¹)	B3LYP-D3	6-31G+(d,p)

Note: Calculations for ECD and OR predictions utilized an implicit (PCM) solvent model for acetonitrile, and calculations for VCD predictions were performed in the gas phase.

incorporated the following SpecDis parameters for UV fitting: a band broadening range of 0.1 to 0.4 eV, a shift range of -30 to +30 nm, and a wavelength range of 180 to 300 nm.

DFT calculations for VCD spectral prediction were performed using the optimal geometry and frequency parameters with Grimme's D3 empirical dispersion correction. All DFT predictions and experimental data were processed based on a maximum IR absorbance of 1. Additionally, DFT calculations were performed on all 152 conformers of (—)-3 to obtain Boltzmann-weighted IR and VCD data in further support of using methyl-truncated

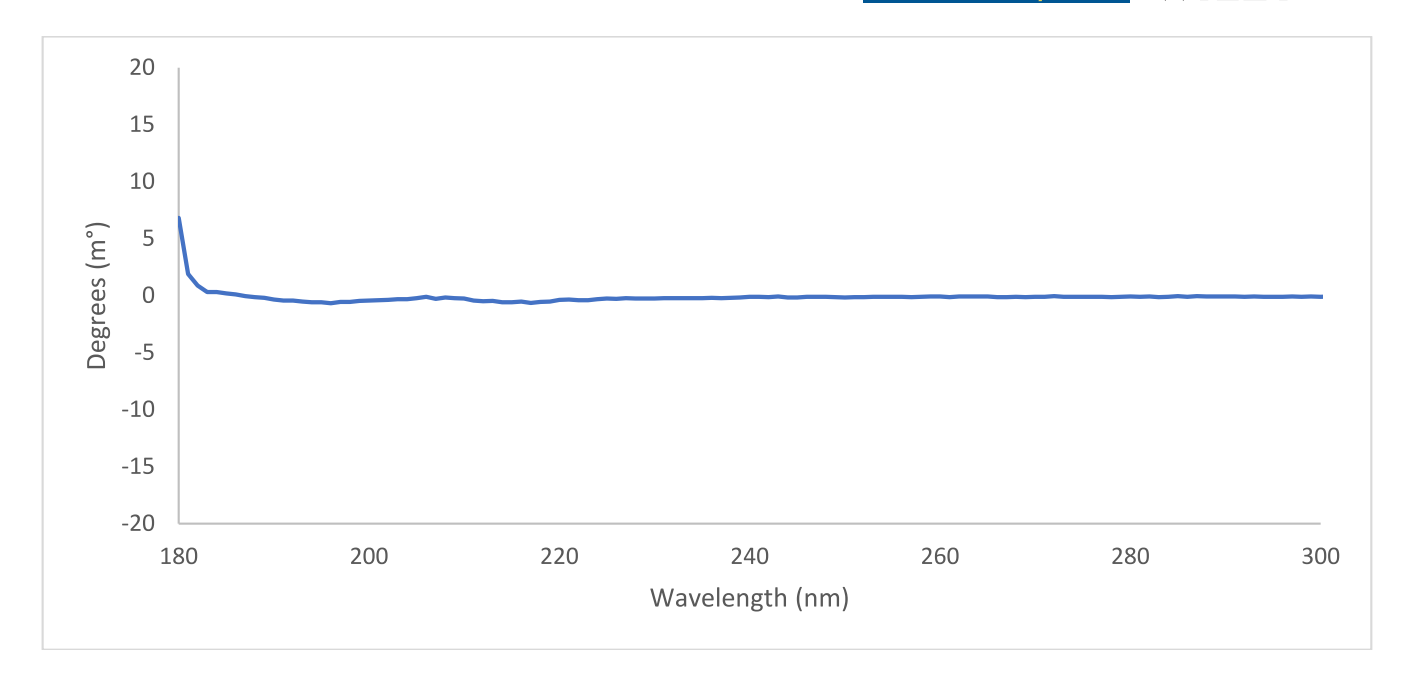


FIGURE 3 An ECD spectrum of CBT-C (3) obtained from a CBD extract.

molecules for related cannabinoid predictions (see Supporting Information).

3 | RESULTS AND DISCUSSION

3.1 | ECD and TDDFT results

An ECD spectrum was acquired after absorbance optimization to facilitate the assignment of CBT-C's (3) absolute configuration. ECD data for CBT-C (3) obtained from a CBD extract displayed a near-flat line (Figure 3), despite literature precedence suggesting the (1*R*,3*R*,4*S*) configuration.^{3,29} A commercial reference standard of CBT-C (3) was obtained, and the experiment was repeated, yielding the same result. This intriguing discovery led to the hypothesis that CBT-C (3) is racemic and that further analysis with chiral-phase HPLC was needed to verify the presence of the two enantiomers.

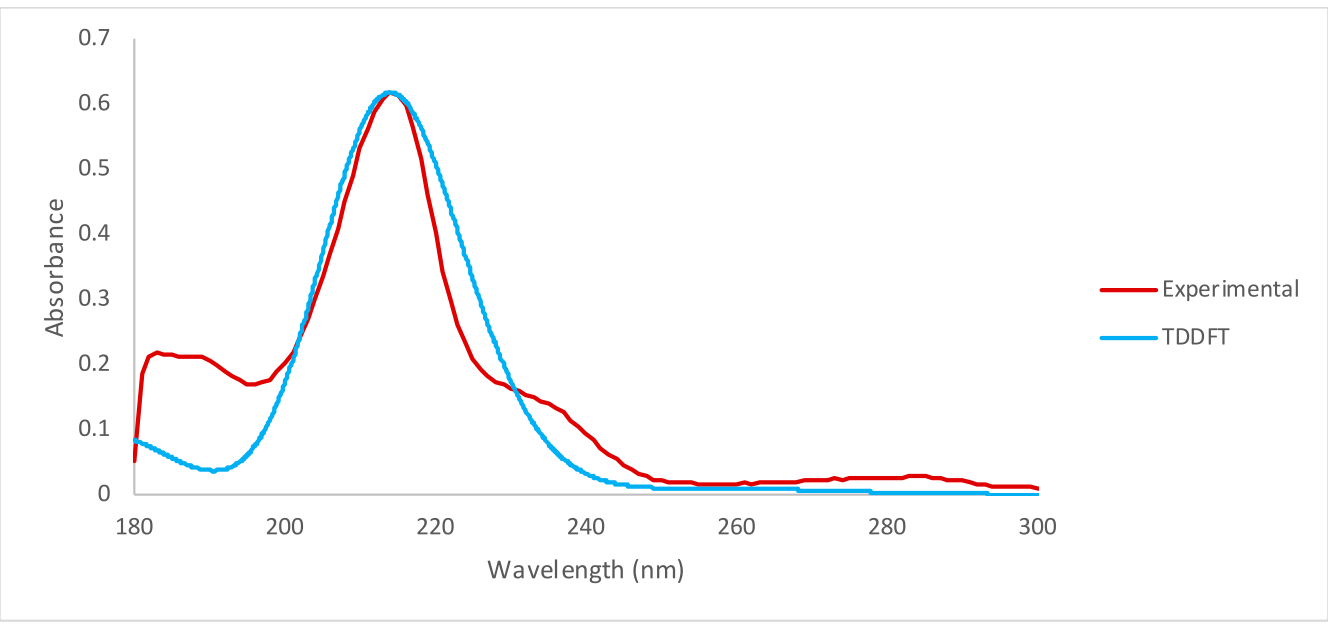
Racemic CBT-C (3) was subjected to HPLC using analytical chiral-phase columns. The CHIRALPAK® IC column efficiently separated the CBT-C (3) enantiomers with equal peak areas. Isolation of individual chromatographic peaks provided microgram quantities of each CBT-C (3) enantiomer. After isolation, ECD experiments were repeated for each enantiomer leading to equal and opposite signals (Figure 4). This separation was successfully scaled up to 1 g using the same stationary phase (250 \times 30 mm column) and elution with 10% MeOH with 0.1% diethylamine/90% CO2 at 90 mL/min 100 bar, with

UV detection at 220 nm and a 1 mL injection volume of a ~50 mg/mL solution.³⁰

Through TDDFT calculations, geometry-optimized methyl-truncated structures of CBT-C (3) enantiomers were used to predict ECD spectra for comparison with experimental data. The resulting predicted UV and ECD spectra for each enantiomer are shown below (Figure 4). Among the various hybrid functionals used, CAM-B3LYP yielded the most accurate results based on wavelength after spectral fitting in SpecDis.

VCD experiments were performed and compared with DFT-predicted data (Figure 5). The results shown are derived from DFT predictions for the methyltruncated structure of CBT-C (3). Comparison of the experimental and DFT-predicted spectra clearly supports the correct configurational assignments of both enantiomers.

The final task was ultimately assigning (–) and (+) to the enantiomers of CBT-C (3) using experimental and TDDFT-predicted OR data. At 589.3 nm, the experimental specific rotation values were measured to be -15 and $+17^{\circ}/(\text{dm} \cdot \text{g/mL})$ in methanol for configurations (1R,3R,4S) and (1S,3S,4R), respectively. These approximately equivalent magnitudes further support the existence of separate enantiomers. Through TDDFT calculations at the ω B97XD/def2-TZVP level of theory, the specific rotation values were predicted to be -21 and $+21^{\circ}/(\text{dm} \cdot \text{g/mL})$ in methanol for configurations (1R,3R,4S) and (1S,3S,4R), respectively. As expected, both CAM-B3LYP and ω B97XD were excellent functionals for



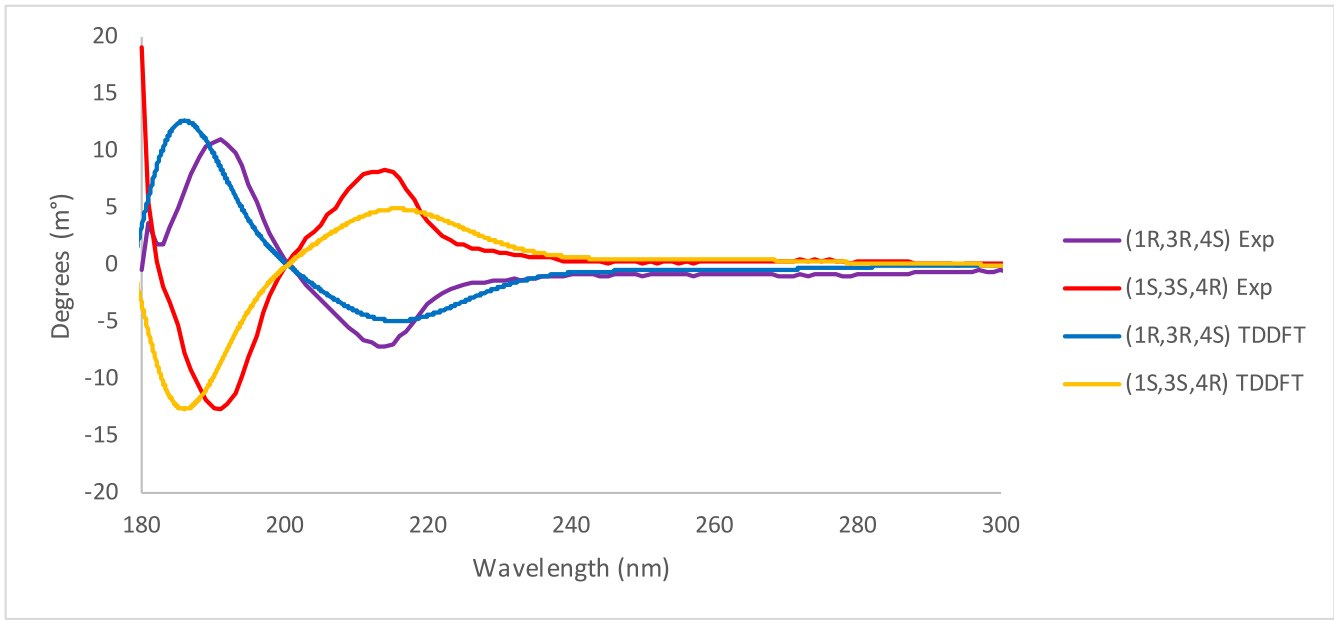


FIGURE 4 Fitted UV and ECD spectra of (-)-3 and (+)-3, including TDDFT results obtained at the CAM-B3LYP/def2-TZVP level of theory.

CBT-C (3) ECD and OR predictions, and def2-TZVP was the best-performing basis set overall (see Supporting Information). It should be noted that while CBT-C (3) has a flexible alkyl chain, OR predictions are known to be more reliable with rigid molecules. However, we have clearly demonstrated that truncation of CBT-C (3) in DFT and TDDFT calculations yields excellent and reliable results, and high accuracy of predicted specific rotations is not necessary for the assignment of (-) and (+) to the individual enantiomers. The mathematical signs of TDDFT-predicted specific rotation values and related cannabinoids (i.e., Δ^9 -cis-THC (1)) provide valuable

support for the correct assignment of the enantiomers' absolute configurations. Thus, configuration (1R,3R,4S) is (-)-CBT-C ((-)-3) and configuration (1S,3S,4R) is (+)-CBT-C ((+)-3).

3.2 | Potential origins of CBT-C

The racemic nature of cannabicitran raised questions about its presumed enzymatic origin. In one example related to a potential biosynthetic origin of CBT-C (3), Schafroth et al. explored the occurrence and chirality of

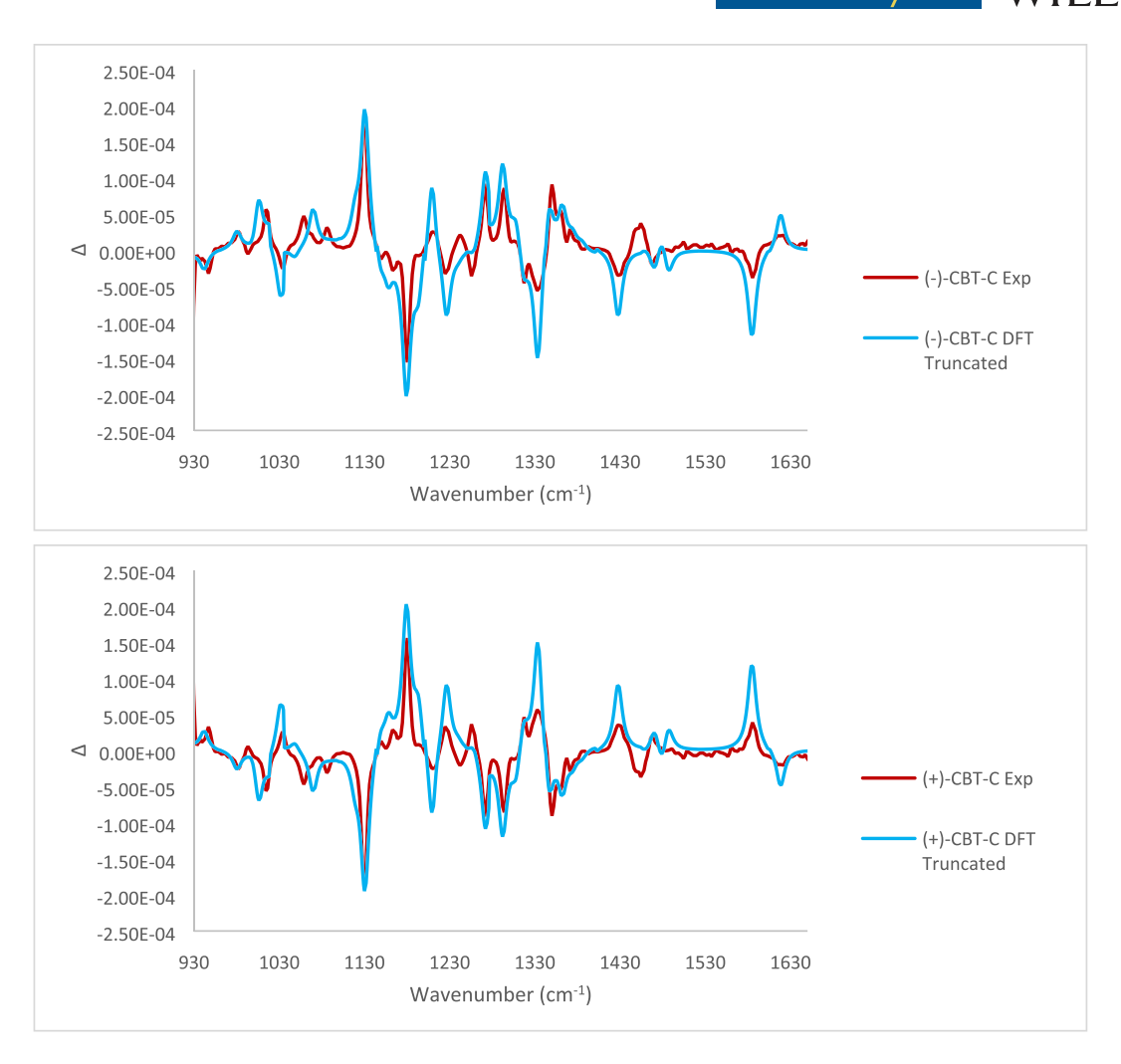


FIGURE 5 Experimental and DFT-predicted VCD spectra for enantiomers of CBT-C (3).

 Δ^9 -cis-THC (1).³ In their report, the presence of Δ^9 -cis-THC (1) was detected quantitatively through chromatography methods in various cannabis fiber hemp strains. It was suggested that biogenetic relationships exist between Δ^9 -cis-THC (1) and trans-CBD (2), as well as CBC (4), which is known to naturally exist as either scalemic or racemic in plants; this is likely due to the nature of its reversible electrocyclization.³² Results from both gas chromatography (GC) and reverse-phase ultrahighliquid performance chromatography (RP-UHPLC) coupled with high resolution mass spectrometry (MS) unambiguously confirmed that both (\pm) - Δ^9 -cis-THCs (1) and (\pm) - Δ^9 -trans-THC (5) co-occur as scalemic mixtures in cannabis fiber hemp strains. Their findings supported our original hypothesis in which CBT-C (3) could originate from Δ^9 -cis-THC (1). Alternatively, it could be suggested that CBT-C (3) is a derivative of CBC (4), which may have a biogenetic relationship with Δ^9 cis-THC (1, Scheme 1). Both compounds are potentially derived from alternative pericyclic processes starting with

CBGA (6) and could be tied to the production of CBT-C (3). The latter could be framed in both enzymatic and nonenzymatic scenarios. An initial oxidation of CBGA (6) yields quinone methide intermediates 7Z and 7E. Intermediate 7Z can undergo a 6π electrocyclization, followed by decarboxylation to generate CBC (4). Alternatively, intermediate 7E reacts via an intramolecular hetero-Diels–Alder cycloaddition followed by decarboxylation to produce Δ^9 -cis-THC (1). CBT-C (3) could potentially be derived from either of the two routes (note: a structural reorientation occurs between 4 and 3).

There is also synthetic evidence suggesting the nonenzymatic formation of CBT-C (3). In the total syntheses of cannabicyclol reported by Yeom et al., a CBT-C (3) analog was formed as a side product through an oxa-[3 + 3] annulation of phloroglucinol and citral.²⁹ The reaction primarily produced a CBC (4) derivative in 93% yield which readily converted to the respective CBT-C (3) analog upon sitting in CDCl₃ at room temperature. It is also noteworthy that findings by Micalizzi et al. confirmed the

SCHEME 1 Potential biosynthetic routes for the production of CBT-C (3) derived from CBGA (6).

presence of CBT-C (3) in dried cultivars of Kompolti and Futura and a lack thereof in fresh cultivars.³³ This may suggest a nonenzymatic formation of CBT-C (3) through the drying process for plant material.

Lastly, it should be noted that in the prior work reported by Iwata and Kitanaka, analogs of both CBC (4) and CBT-C (3) were extracted and isolated from Rhododendron anthopogonoides, which is known to contain analogs of CBC (4) and other cannabinoids.34 Our findings contrast with those of Iwata and Kitanaka, whose ECD data were reportedly in correspondence with a methyl-truncated (+)-3 analog. It was expected that the ECD spectrum of the (+)-3 analog should display key similarities to our experimental data. Provided the synchronous presence of both CBC (4) and CBT-C (3) in common sources, it is possible that the presented analog of (+)-3 is correct, but the respective ECD spectrum was not consistent with our experimental and calculated data. No corresponding NMR data were presented in this report to unify structural characterization of the molecule with the reported ECD spectrum. These cumulative findings support the possibility that "natural" CBT-C (3) is in fact formed through the process of extraction from raw plant material and that CBC (4) is a viable precursor molecule involved in the formation of CBT-C (3).

4 | CONCLUSIONS

Through ECD, VCD, and OR analysis, it can be concluded that CBT-C (3) isolated from cannabinoid extracts is racemic. The CBT-C (3) enantiomers can be resolved by HPLC using the CHIRALPAK® IC column, where (-)-3 elutes before (+)-3 with significant resolution. The (-) and (+) enantiomers possess the (1R,3R,4S) and (1S,3S,4R) configurations, respectively. We recommend performing ECD TDDFT calculations for general cannabinoids at the CAM-B3LYP/def2-TZVP//B3LYP/6-31G +(d,p) level of theory and OR TDDFT calculations at the ωB97XD/def2-TZVP//B3LYP/6-31G+(d,p) level of theory. The use of Grimme's D3 empirical dispersion correction in VCD predictions yielded excellent results. Future efforts will include improved access to single enantiomer CBT-C (3) and corresponding pharmaceutical applications of each enantiomer.

ACKNOWLEDGMENTS

We would like to acknowledge Dr. Xiao Wang and Ryan D. Cohen for helpful discussions and the Yousry and Linda Sayed Endowment for funding.

DATA AVAILABILITY STATEMENT

Data that support this study are openly available in the Supporting Information of this article or are available from the corresponding authors upon reasonable request.

ORCID

R. Thomas Williamson https://orcid.org/0000-0001-7450-3135

REFERENCES

- Vučković S, Srebro D, Vujović KS, Vučetić Č, Prostran M. Cannabinoids and pain: new insights from old molecules. Front Pharmacol. 2018;9:1259. doi:10.3389/fphar.2018.01259
- Zou S, Kumar U. Cannabinoid receptors and the endocannabinoid system: signaling and function in the central nervous system. *Int J Mol Sci.* 2018;19(3):833. doi:10.3390/ijms19030833
- Schafroth MA, Mazzoccanti G, Reynoso-Moreno I, et al. Δ⁹-cis-Tetrahydrocannabinol: natural occurrence, chirality, and pharmacology. J Nat Prod. 2021;84:2502-2510. doi:10.1021/acs. jnatprod.1c00513
- 4. Morales P, Reggio PH, Jagerovic N. An overview on medicinal chemistry of synthetic and natural derivatives of cannabidiol. *Front Pharmacol.* 2017;8:422. doi:10.3389/fphar.2017.00422
- Bisogno T, Hanuš L, Petrocellis LD, et al. Molecular targets for cannabidiol and its synthetic analogues: effect on vanilloid VR1 receptors and on the cellular uptake and enzymatic hydrolysis of anandamide. *Br J Pharmacol*. 2009;134(4):845-852. doi: 10.1038/sj.bjp.0704327
- 6. Kim JH, Scialli AR. Thalidomide: the tragedy of birth defects and the effective treatment of disease. *Tox Sci.* 2011;122:1-6. doi:10.1093/toxsci/kfr088

9

- 7. Nguyen LA, He H, Pham-Huy C. Chiral drugs: an overview. *Int J Biomed Sci.* 2006;2:85-100. https://www.ncbi.nlm.nih.gov/pubmed/23674971
- Rehman W, Arfons LM, Lazarus HM. The rise, fall and subsequent triumph of thalidomide: lessons learned in drug development. *Ther Adv Hematol*. 2011;2(5):291-308. doi:10.1177/2040620711413165
- Knoche B, Blaschke G. Investigations on the in vitro racemization of thalidomide by high-performance liquid chromatography. *J Chromatogr*. 1994;666:235-240. doi:10.1016/0021-9673 (94)80385-4
- 10. Eliel EL. Infelicitous stereochemical nomenclature. *Chirality*. 1997;9(5-6):428-430. doi:10.1002/(SICI)1520-636X(1997)9:5/6% 3C428::AID-CHIR5%3E3.0.CO;2-1
- 11. Burke WJ, Kratochvil CJ. Stereoisomers in psychiatry: the case of escitalopram. *Prim Care Companion J Clin Psychiatry*. 2002; 4(1):20-24. doi:10.4088/pcc.v04n0107
- Zask A, Ellestad GA. Reflections on the intriguing occurrence of some recently isolated natural products as racemates and scalemic mixtures. *Chirality*. 2021;33:915-930. doi:10.1002/chir. 23360
- Batista ANL, dos Santos FM, Batista JM, Cass QB. Enantiomeric mixtures in natural product chemistry: separation and absolute configuration assignment. *Molecules*. 2018;23(2):492. doi:10.3390/molecules23020492
- 14. Bitchagno GTM, Nchiozem-Ngnitedem V-A, Melchert D, Fobofou SA. Demystifying racemic natural products in the homochiral world. *Nat Rev Chem.* 2022;6(11):806-822. doi:10. 1038/s41570-022-00431-4
- Vu V-T, Chen X-L, Kong L-Y, Luo J-G. Melipatulinones A-C, three lignan-phloroglucinol hybrids from *Melicope patuliner-via*. *Org Lett*. 2020;22:1380-1384. doi:10.1021/acs.orglett. 9b04680
- de Almeida DL, Devi LA. Diversity of molecular targets and signaling pathways for CBD. *Pharmacol Res Perspect*. 2020;8(6): e00682. doi:10.1002/prp2.682
- Fasinu PS, Phillips S, ElSohly MA, Walker LA. Current status and prospects for cannabidiol preparations as new therapeutic agents. *Pharmacotherapy*. 2016;36:781-796. doi:10.1002/phar. 1780
- 18. Wood JS, Gordon WH, Morgan JB, Williamson RT. Calculated and experimental ¹H and ¹³C NMR assignments for cannabicitran. *Magn Reson Chem.* 2021;60:196-202. doi:10.1002/mrc. 5224
- 19. Wilson G, John B, Miller R. Cannabinoid sunscreen formulations. U.S. Patent WO 2021207182. October 14, 2021.
- Persaud A. Cannabinoid-comprising cosmetic compositions.
 U.S. Patent WO 2021224693. November 11, 2021.
- 21. Meiri D, Aviram J. Compositions and methods for treating headaches. U.S. Patent WO 2021245658. December 9, 2021.
- 22. Trambitas DO, Woerlee GF. Food supplement for Alzheimer disease. U.S. Patent WO 2021130002. July 1, 2021.
- 23. ElSohly MA, Harland EC, Benigni DA, Waller CW. Cannabinoids in glaucoma II: the effect of different cannabinoids on intraocular pressure of the rabbit. *Curr Eye Res.* 1984;3:841-850. doi:10.3109/02713688409000797
- 24. McHugh D, Hu SS, Rimmerman N, et al. *N*-arachidonoyl glycine, an abundant endogenous lipid, potently drives directed

- cellular migration through GPR18, the putative abnormal cannabidiol receptor. *BMC Neurosci.* 2010;11:44. doi:10.1186/1471-2202-11-44
- Ramírez-Orozco RE, García-Ruiz R, Morales P, Villalón CM, Villafán-Bernal JR, Marichal-Cancino BA. Potential metabolic and behavioural roles of the putative endocannabinoid receptors GPR18, GPR55 and GPR119 in feeding. *Curr Neuropharmacol*. 2019;17(10):947-960. doi:10.2174/1570159X17666190118143014
- 26. Qin Y, Verdegaal EME, Siderius M, et al. Quantitative expression profiling of G-protein-coupled receptors (GPCRs) in metastatic melanoma: the constitutively active orphan GPCR GPR18 as novel drug target. *Pigment Cell Melanoma Res.* 2010; 24:207-218. doi:10.1111/j.1755-148X.2010.00781.x
- Lu C, Wu C, Ghoreishi D, et al. OPLS4: improving force field accuracy on challenging regimes of chemical space. *J Chem Theory Comput.* 2021;17:4291-4300. doi:10.1021/acs.jctc. 1c00302
- 28. Bruhn T, Schaumlöffel A, Hemberger Y, Pecitelli G. SpecDis version 1.71, Berlin, Germany. 2017. https://specdis-software.jimdo.com
- 29. Yeom H-S, Li H, Tang Y, Hsung RP. Total syntheses of cannabicyclol, clusiacyclol A and B, iso-eriobrucinol A and B, and eriobrucinol. *Org Lett.* 2013;15:3130-3133. doi:10.1021/ol401335u
- 30. Lotus Separations, LLC. http://www.lotussep.com/
- 31. Stevens PJ, McCann DM, Cheeseman JR, Frisch MJ. Determination of absolute configurations of chiral molecules using ab initio time-dependent density functional theory calculations of optical rotation: how reliable are absolute configurations obtained for molecules with small rotations? *Chirality*. 2005;17: S52-S64. doi:10.1002/chir.20109
- Novak AJE, Trauner D. Reflections on racemic natural products. *Trends Chem.* 2020;2:1052-1065. doi:10.1016/j.trechm. 2020.10.005
- 33. Micalizzi G, Alibrando F, Vento F, et al. Development of a novel microwave distillation technique for the isolation of *Can*nabis sativa L. essential oil and gas chromatography analyses for the comprehensive characterization of terpenes and terpenoids, including their enantio-distribution. *Molecules*. 2021;26: 1588. doi:10.3390/molecules26061588
- 34. Iwata N, Kitanaka S. New cannabinoid-like chromane and chromene derivatives from *Rhododendron anthopogonoides*. *Chem Pharm Bull (Tokyo)*. 2011;59:1409-1412. doi:10.1248/cpb. 59.1409

SUPPORTING INFORMATION

Additional supporting information can be found online in the Supporting Information section at the end of this article.

How to cite this article: Wood JS, Gordon WH, Morgan JB, Williamson RT. Cannabicitran: Its unexpected racemic nature and potential origins. *Chirality.* 2023;1-9. doi:10.1002/chir.23571